Comparison between different lines reveals that Ipomoea cairica (L.) in mangrove wetlands acquires the ability to resist salt through phenotypic plasticity

Jiatong Zou
South China Normal University
Benqi Yuan
South China Normal University
Weihua Li
South China Normal University
xiaoting Xie
South China Normal University
Minghao Chen
South China Normal University
Tiantian Xiong (xiongtiantian@m.scnu.edu.cn)
South China Normal University https://orcid.org/0000-0002-1850-0287

Research Article

Keywords: Invasive plant, Morning glory Ipomoea cairica (L.) Sweet, Antioxidant activity, Ion homeostasis, Ecological adaptation, Salt stress

Posted Date: November 14th, 2023

DOI: https://doi.org/10.21203/rs.3.rs-3417629/v1

Abstract

Palmate-leaved morning glory (*Ipomoea cairica* (L.) Sweet) is a fast-growing perennial herbaceous twining vine that was recently discovered to invade mangrove wetlands in China. To understand the mechanism of its successful invasion, we compared the salt tolerance of a halophytic line from Zhuhai and a non-halophytic line from Guangzhou under salt stress. We measured morphological, physiological, and biochemical parameters related to growth, ion homeostasis, photosynthetic pigments, chlorophyll fluorescence parameters, oxidative stress, and apoptosis in both lines. Monitoring apoptosis showed that the halophytic line had a delayed protoplast apoptosis compared with the non-halophytic line. We also found that the halophytic line had higher stems that regenerated; lower water loss, Na^+ uptake, and membrane damage; a higher density and area of salt glands; and better photosynthetic performance than the non-halophytic line. The halophyte prevented salt-related damage by reducing water loss and secreting excess sodium ions (Na^+) through its lower stomatal density and higher density and area of salt glands. The halophytic line also maintained a better balance of Na^+, potassium ions, nitrogen, and phosphorus under salt stress. The halophytic line had higher activities of antioxidant enzymes, including superoxide dismutase, peroxidase, and catalase, and non-enzymatic antioxidants of proline and anthocyanins, which indicate a stronger oxidative stress response. Our results suggest that the halophytic line adapts to higher salt tolerance than the non-halophytic line by enhancing its salt exclusion, osmolyte adjustment, and photosynthetic efficiency, which could explain its successful invasion in the mangrove wetland ecosystem.

Introduction

A rapidly growing number of alien invasive species is causing increasing damage to China's agriculture, forestry, and livestock industries (Ding Hui et al. 2009) with annual economic losses that exceed $100 billion (Gu et al. 2006). In hotspots of introduced species, such as coastal zones, biological invasions are becoming a major driver of the decline of biodiversity and loss of ecological services in communities, such as coastal forests (Bellard et al. 2016; Slingsby et al. 2017). Mangroves are unique higher plant communities that are widely distributed in the intertidal zones of tropical and subtropical regions. They are unique wetland forest ecosystems in the coastal zone. With high productivity and biodiversity, the abundance of biological resources and species in the mangrove wetland ecosystem is among the highest in the natural environment (Lin et al. 1997; Saenger et al. 2019; Wang et al. 2022). However, the mangrove wetland ecosystem has been severely degraded, and one of the reasons for the degradation is the invasion of alien species, including smooth cordgrass (*Spartina alterniflora*) and bitter vine (*Mikania micrantha*) (Jackson et al. 2001; Biswas et al. 2007; Guan et al. 2011; Ren et al. 2014; Zhang et al. 2021). Palmate-leaved morning glory (*Ipomoea cairica*) is a typical invasive plant in South China, which has caused severe damage to ecosystems and local economies (Liu et al. 2012; Zhu and Shuangtao 2012). This plant has been listed as one of the worst invasive alien species in China (Bai et al. 2013). In our previous study, *I. cairica* was reported to invade mangroves along the southeastern coast of China (Liu et al. 2012; Yuan et al. 2020). Compared with other habitats, the soil of mangroves is more

saline (Chen and Xu 2007; Yokoi et al. 2012; Morimaru et al. 2017; Fu et al. 2022). Therefore, salt tolerance is a limiting factor for invasive plants to invade mangroves.

The most extensive and profound effect of an external salt environment on plants is to inhibit plant growth and development (Munns and Tester 2008; Naz et al. 2022). For example, salt alters many functional and biochemical processes in plants, which can lead to reduced growth, productivity, and even death. Tissue dehydration, ion-specific toxicity, nutrient shortages, and hormonal/enzymatic imbalances are the primary mechanisms that are affected by salt stress (Polash et al. 2019; Zeeshan et al. 2020; Wei et al. 2022). As a result, salt stress leads to a variety of physiological and molecular changes and impedes plant growth by impairing photosynthesis, which reduces the resources available and suppresses cell division and expansion (Hao et al. 2021). Photosynthesis is the primary driver for plant growth and development and is one of the physiological processes of plants that is the most sensitive to stress (Lawlor 1995; Yang et al. 2009; Allakhverdiev 2020). Changes in photosynthesis are directly related to the chlorophyll fluorescence parameters of photosystem II (PSII) (Guo et al. 2001). Analysis of the chlorophyll fluorescence parameters can rapidly determine the photochemical efficiency of plant PSII without damage, and it is an important method to diagnose whether PSII is functional and analyze the mechanism of plant's response to stress (Baker and Rosenqvist 2004; Baker 2008). Therefore, monitoring different chlorophyll fluorescence parameters can provide important information on changes in the plant photosynthetic dynamics under a wide range of environmental stresses (Baker 2004). The osmotic potential is another important indicator that is related to salt stress (Blum 2017; Hessini et al. 2019). When the osmotic potential in the plant exceeds the external environment, it is difficult for the plant to absorb enough water, which causes a physiological water shortage in the plant, also known as osmotic stress (Zhu 2016). Salt tolerance in plants is implemented at both the organ and cellular levels. The stomata play a key role in the survival of plants in adverse environments. A reduction in stomatal density may delay the accumulation of toxic ions and signaling molecules that inhibit growth in the leaves through a reduced transpiration flow under salt stress, thus, facilitate adaptation to salinity stress (Barbieri et al. 2012; Orsini et al. 2012; Hasanuzzaman et al. 2023). Salt glands actively secrete excessive amounts of ions out of the plant cells to avoid toxicity (Yuan, Leng, and Wang 2016).

Previous research on *I. cairica* has primarily focused on its invasion in terrestrial ecosystems. *I. cairica* has high rates of stem growth and photosynthesis, can reproduce asexually, and grows vegetatively (Huang et al. 2008; Shen et al. 2011; Liu et al. 2012; Hou et al. 2014; Yu and Li 2019). Compared with native companion species, *I. cairica* is more resistant to abiotic stressors, such as heat and drought resistance among others, which enables it to rapidly invade tropical and subtropical terrestrial ecosystems (Wu et al. 2004; Zhu et al. 2009; Wang et al. 2011; Tognon et al. 2012; Chen et al. 2022). The stress resistance of *I. cairica* primarily originates from its high antioxidant capacity and stability of its photosynthetic system. Under adverse conditions, *I. cairica* enhances its antioxidant capacity by overexpressing *IcSRO1* (SIMILAR TO RCD-One), while enhancing its photosynthetic system stability by overexpressing *IcOr* (ORANGE) (Yuan et al. 2020; Chen et al. 2022). However, the mechanism of its invasion in coastal wetland ecosystems remains unknown. Therefore, understanding the responses of *I.*

cairica to salt stress and its associated mechanisms of tolerance may help explain its adaptation to mangrove wetlands.

In this study, we investigated halophyte lines in the mangrove wetland ecosystem and non-halophyte lines in the inland ecosystem and compared their responses to salt stress. The results provide evidence for how *I. cairica* maintains its ability to invade during the process of diffusing from non-salt to salt habitats.

Materials and methods

Plant material and growth conditions

The non-halophytic line of *I. cairica* was collected from the Biological Park of South China Normal University, Tianhe District, Guangzhou City, China (23.13 ° N, 113.35 ° E). The halophytic line of *I. cairica* was collected from the Qi'ao Mangrove Wetland Park in Gaoxin District, Zhuhai City, China (22.43 ° N, 113.62 ° E). Stems of *I. cairica* that were 10 cm long and had two nodes were selected for cultivation in one-half Hoagland nutrient solution (pH = 5.7) that contained 0.48 mmol/L, 50 mmol/L and 100 mmol/L of Na^+ (Hoagland &Arnon, 1950). NaCl was used to provide Na^+, and the control was treated in this manner. The solution was updated every 4 d. After 2 weeks of cultivation, the root lengths were measured. Seedlings cultivated in 0.48 mmol/L Na^+ were transplanted into flowerpots that contained clean sand that had been filtered through a 10-mesh sieve. One-half Hoagland nutrient solution (150 mmol/L Na^+) was used for the salt treatments, while 0.48 mmol/L Na^+ was used for the control.

Plant harvest and growth parameters

Nondestructive growth parameters, including the root length, tendency of the main stem to grow, leaf number during the salt treatment, branch number, and number of flowers, were measured every 10 days for a total of 60 days. The plant harvest and growth parameters were measured as described by Luo et al. (2021) and Kumar et al. (2021). After harvest, the fresh weight (FW) of the aboveground parts and roots was determined. The enzymes in the plant tissue were inactivated by heating at 105°C for 40 min and then drying to a constant weight at 75°C for 12 h to calculate the dry weight (DW). The water content (WC) was calculated using the following formula: WC = (FW – DW)/ FW × 100. Furthermore, the root to shoot ratio was calculated by the root dry weight/shoot dry weight as previously described (Luo et al. 2021).

Detection of apoptosis

Four-week-old leaves of *I. cairica* were obtained and cut into strips of 0.74–1.25 mm, immersed in an enzymolysis solution, and digested for 5–6 hours. The digestive solution that was obtained was passed through a 50 μm sieve, washed with 0.5 M mannitol, and purified in 15% sucrose. The protoplasts were resuspended in modified KM8P liquid media (Kao and Michayluk, 1974). Cell apoptosis was detected

through Annexin V-FITC/PI (Sangon Biotech (Shanghai) Co., Ltd., Shanghai, China) double staining flow cytometry (Galbraith et al. 1983; Dong et al. 2017).

Detection of membrane integrity in the root cells

Membrane integrity in the *I. cairica* root cells was detected using a slightly modified method described by Lequeux et al. (2010). The roots of the two *I. cairica* lines in Guangzhou and Zhuhai were treated with 100 mmol/L NaCl for 12 h, stained with 0.25% Evans blue solution for 15 min, and then washed three times with ultrapure water before they were photographed. The surface of these roots after staining with Evans blue was observed under a microscope (DM3000, Leica, Wetzlar, Germany). The roots were immersed in 3 mL of pure N, N-dimethylformamide (N, N-dimethylformamide, DMF, analytical grade [Sigma-Aldrich, St. Louis, MO, USA]) for 30 min, and the absorbance of the extract at 600 nm was measured by spectroscopy (DU730 UV/Vis Spectrophotometer, Beckman Coulter Inc., Brea, CA, USA).

Determination of the content of proline (Pro)

The Pro was measured as described by Shi et al. (2016). A total of 0.1 g of sample was added to 3 mL of 3% sulfosalicylic acid, incubated for 10 min in a boiling water bath, and then cooled and centrifuged at 6,000 g for 10 min. After that, 1 mL of the supernatant was collected and mixed with 4 mL of extraction buffer (distilled water: glacial acetic acid: acidic ninhydrin = 1:1:2). The mixture was boiled for 1 h and cooled at room temperature. After that, 2 mL of toluene was added, and the phases were left to separate for 2 h. After full extraction, the red toluene phase was subjected to a colorimetric analysis at 520 nm. The content of Pro was calculated from a standard curve.

Determination of the absorption spectrum and content of anthocyanins in the leaves

The leaves of *I. cairica* were extracted in HCl: MeOH: H_2O (1:1:98) at 4 ℃ for 12 h and then centrifuged at 4500 rpm for 5 min. The absorption spectrum of the supernatant was scanned from 400 nm to 700 nm. The absorption values at 535 nm and 650 nm were recorded. The total content of anthocyanins in the leaves was calculated using the standard anthocyanin-3-glucose (extinction coefficient [$(31.6\ mmol \cdot L^{-1})^{-1}\ cm^{-1}$]) (Hoch et al. 2003).

Determination of the antioxidant enzyme activities

The antioxidant enzymes were extracted from 0.1 g of leaves as described by Zhang et al. (2021). Peroxidase (POD) and superoxide dismutase (SOD) were assayed as described by Chen et al. (2022). The catalase (CAT) was assayed as described by Aebi (1984). The reaction mixture (3 mL) contained 2.9 mL of 30 mM H_2O_2 (Guangzhou Chemical Reagent Factory, Guangzhou, China) and 0.1 mL of enzyme extract. The decrease in absorbance was recorded at 240 nm. One unit of enzyme activity was defined as 1 nmol H_2O_2 dissociated$\cdot min^{-1}$.

Determination of the contents of relative electrical conductivity (REC) and malondialdehyde (MDA)

The REC was measured using a DJS-1D conductivity meter (Leica, Shanghai, China). A total of 0.1 g of leaf material was placed in 10 mL of deionized water in a test tube and soaked for 2 h at 25 ℃ to measure the electrical conductivity R1. After this, the sample was boiled for 30 min, and once the temperature had dropped to room temperature, the conductivity R2 was measured. The content of REC was calculated using the formula R1/R2 × 100% (Cao et al. 2007; Fan et al. 2022). The content of MDA was measured as described by Chen et al. (2022).

Measurement of the chlorophyll fluorescence parameters

After 30 d of treatment, the chlorophyll fluorescence parameters were measured using a portable modulating chlorophyll fluorescence instrument PAM-2500 fluorometer (Walz, Effeltrich, Germany) as described by Chen et al. (2022). Approximately 20 treated seedlings were adapted in the dark for at least 20 min before the chlorophyll fluorescence was assessed. The parameters included the maximum efficiency of PSII photochemistry (Fv/Fm), effective quantum yield of PSII (Y[II]), photochemical quenching coefficient (qL), electron transport rate (ETR) and non-photochemical chlorophyll fluorescence quenching (NPQ). Five replicates per cultivar were assessed from both the treated and control plants.

Measurement of stomatal density

The abaxial leaf surface was coated with clear nail varnish as described by Tao et al. (2021). The dried layer of the nail varnish was then peeled off using tweezers and placed on a glass slide. The imprints were subsequently observed under an optical microscope with a 10x objective. A certain number of pictures of the field of view were taken, and the number of all the stomata in the field of view was counted using ImageJ (NIH, Bethesda, MD, USA). ImageJ was used to calculate the stomatal density (the number of stomata per unit of leaf area in the field of view) with the number of stomata/the area of the field of view (0.1590 mm^2). The sample size for each treatment and genotype was 75 (three epidermal samples per leaf × five fields of view per sample × five biological replicates). The highest and lowest values were discarded in the analyses, and the remaining data were averaged.

Measurement of the density and area of salt glands

In combination with a slight modification of a previous method (Tao et al. 2021), the back of leaf blade was coated with clear nail polish. The dried nail polish layer was then peeled off with tweezers and placed on a glass slide. These blotches were then observed under a 5× objective light microscope, and the field of view was photographed many times. The number of all the salt glands in the field of view and the area of the salt glands were counted using ImageJ, which was used to calculate the density of salt glands (the total number of salt glands per unit leaf area in the field of view) and their area as previously described (Yuan et al. 2022; Zhao et al. 2023).

The density of salt glands was calculated as the total number of salt glands divided by the leaf area of six replicate observations as described by Ding et al. (2010) and Leng et al. (2018). There were 35 samples per treatment and line (seven fields of view per biological replicate × five biological replicates).

The total area of salt glands was measured using ImageJ for 15 individual salt glands at different locations with a sample size of 75 per treatment and line (five biological replicates per treatment, five fields of view per biological replicate, and five fields of view for a total of 15 total salt glands).

Determination of the contents of nitrogen, phosphorus, potassium, and sodium in the roots, stems, and leaves

After 60 d of cultivation, the plants were harvested and divided into three parts, including the roots, stems, and leaves. All the materials were heated for 1.5 h at 110 ℃ and at 75 ℃ for 2 d until stable. The shoots and roots were crushed and passed through a 20-mesh sieve. After dehydration, carbonization, and oxidation by digesting with H_2SO_4·H_2O_2 as previously described (Smith 1979), the organic matter in the sample was destroyed and transformed to inorganic salts. After dilution with acid, an atomic absorption spectrophotometer (AA-7000, Shimadzu Corporation, Kyoto, Japan) was used to measure the contents of N, P, potassium, and sodium in each sample.

Statistical analysis

All the experiments in this study were repeated three times independently, and the values are shown as the mean ± SD. The data were analyzed using a one-way analysis of variance (ANOVA) or two-way ANOVA. The subsequent multiple comparisons were examined based on the least significant difference (LSD) test. $P < 0.05$ was considered a significant level. The data were analyzed using SPSS 21.0 (IBM, Inc., Armonk, NY, USA). The figures were prepared using Origin 2019 (OriginLab, Northampton, MA, USA).

Results

Growth of the two lines under salt stress

With the increase in the concentration of salt treatment, the rooting length of the non-halophytic line decreased significantly (Fig. 1a–b). To track the growth of two lines under salt stress, the seedlings were treated with salt after transplantation, and the stem length, number of leaves, number of branches and number of flowers of each plant were assessed (Fig. 1c–f). After 10 d, the stems of the halophytic line under salt treatment were significantly shorter than those in the control group. In the control group, the stems of non-halophytic lines gradually grew longer. At 50 d, the main stem length from longest to shortest was significantly different between the non-halophytic line in the control, the halophytic line in the control, the halophytic line in the saline treatment, and the non-halophytic line in the saline treatment (Fig. 1c). After 20 d, there were significantly more leaves in the control group than in the salt treatment, but there was no significant difference between the non-halophytic and the halophytic lines in both the control and salt treatments (Fig. 1d). At 20 d, the halophytic line in the control group flowered first. At the end of the experiment, there were significantly more flowers in the control group of the halophytic lines than in the salt treatment. In contrast, there was no difference in the number of flowers between the control and salt treatment in the non-halophytic lines (Fig. 1f). Under salt treatment, there were

significantly more branches in the non-halophytic line than in the halophytic line. However, there was no significant difference between the two lines in the control group (Fig. 1e). The analytical results indicated that the halophytic and non-halophytic lines may have adapted to their respective habitats. The non-halophytic line is more adapted to the non-salt environment, while the halophytic line is more adapted to the saline environment.

The elevated concentration of NaCl significantly inhibited the growth of non-halophytic and halophytic lines (Fig. 2a–d). The halophytes grew better than the non-halophytes in both the control and treatment groups. There was no significant difference between the two lines, but the roots of the non-halophytic line were more sensitive to salt, and their root FW was lower in the non-halophytic lines than in the halophytic lines under the salt treatment (Fig. 2e). In addition, the elevated concentration of NaCl had a greater impact on the aboveground biomass and total biomass of the non-halophytic line, with rates of inhibition of 43% and 45%, respectively. In contrast, the rates of inhibition of the aboveground biomass and total biomass of the halophytic line by the elevated concentration of NaCl were 31% and 37%, respectively (Fig. 2f–g). In terms of water content, the halophytic line differed from the non-halophytic line by a significantly lower decrease after the salt treatment compared with their controls. The halophytic line exposed to salinity had a significantly higher root-to-shoot ratio than its competitor. In contrast, there was no detectable difference in the control groups (Fig. 2h–i).

Effect of salt stress on the chlorophyll content and fluorescence characteristics of the two lines

The contents of total Chl, Chl a, and Chl b decreased to 69% and 73%, 67% and 74%, and 73% and 71% of the control, respectively, after the salt treatment. In addition, the halophyte had higher contents than the non-halophyte in both the control and salt treatments, but the differences were not significant. The halophyte had a higher Chl a/Chl b ratio than the non-halophyte after the salt treatment (Fig. 3a-d).

As shown in Fig. 3e, the Fv/Fm remained stable across both lines under both treatments. Under the salt treatment, the external quantum yield of PS II (Y[II]) of both the non-halophyte and the halophyte decreased significantly by 35.54% and 29.03%, respectively, when compared with the control (Fig. 3f). The qL decreased by 16.67% and 10.63% in the non-halogenated and halogenated plants, respectively, compared with the control. However, there was no significant difference between the control and salt treatments (Fig. 3g). Under the salt treatment, the NPQ of two lines increased (Fig. 3h). The ETR of both the non-halophyte and the halophyte in the salt treatment decreased significantly compared with the corresponding controls; the ETR of the non-halophyte decreased by 35.31%, and that of the halophyte decreased by 28.97% (Fig. 3i).

Cell damage of the two lines under salt stress

Apoptosis of the leaf protoplast was induced in both lines under salt stress. The non-halophytic line entered the apoptosis stage earlier than the halophytic line (Fig. 4a-b). Evans blue staining was used to explore the effect of salt stress on the membrane integrity of the root cells. After 12 h of treatment, the non-halophyte displayed a darker blue stain on the root tip than the halophyte, which suggested that there

was more severe cell damage. The values of absorbance of the decolorizing solution at 600 nm indicated that the non-halophyte suffered greater damage to the cell membrane than the halophyte under salt stress (Fig. 4c-d). The contents of MDA and REC of the non-halophyte were higher than those of the halophyte under both the control and salt treatments. Furthermore, the contents of MDA and REC of the non-halophyte were significantly higher than those of the halophyte in the salt treatment (Fig. 4e-f).

Antioxidant capacity of *I. cairica* in response to salt stress

The content of Pro in the halophyte was higher than that of the non-halophyte under both the control and salt treatments, while the content in the halophyte was significantly higher than that of the non-halophyte in the salt treatment (Fig. 5a). Under the control treatment, the halophyte appeared to accumulate significantly more anthocyanins than the non-halophyte. The halophyte had a concentration of anthocyanins that was approximately twice as high. However, there was no significant difference between the two lines under the salt treatment since the anthocyanin content of the non-halophytic increased significantly compared with its control (Fig. 5b). The SOD activity of the halophyte under both the control or salt treatment was significantly higher than that of the non-halophyte. However, the activity of both lines increased under salt treatment (Fig. 5c). The POD activity of the halophyte in the control group was significantly higher than that of the non-halophyte, and the activity in the salt treatment group increased in both lines (Fig. 5d). The CAT activity increased in the salt treatment. The activity of the halophyte was higher in the control and salt treatments than in the non-halophyte, but the difference was not significant (Fig. 5e).

Salt gland diameter and density

The appearance of the stomata and salt glands of the two strains were examined in detail, and their associated metrics were determined (Fig. 6a-f, and g-m). In both the control and salt treatments, the number of stomata and stomatal density were higher in the non-halophyte than in the halophyte lines, and a significant difference was observed in the salt treatment group (Fig. 6a-f). There was no significant difference in the area of the salt glands between the two lines in either the control or treatments. However, the area of the salt glands in both lines increased under the salt treatments and was approximately 1.13- and 1.14-fold that of the control, respectively (Fig. 6k). The number and density of the salt glands increased in both lines compared with the control. There was a significant difference in these values between the two lines under the salt treatment, with the halophyte approximately 1.36- and 1.4-fold higher than that of the non-halophyte, respectively. Secondly, in the control, there was no significant difference in the number and density of salt glands between the two lines, but the values for the halophyte were higher than those of the non-halophyte (Fig. 6l-m).

Contents of elements in the roots, stems, and leaves

Under non-saline conditions, significantly less Na^+ accumulated in the roots, stems, and leaves of the halophyte compared with the non-halophyte. Na^+ was absorbed by the roots in excess when the plants were exposed to salt, and this significantly increased the concentration of Na^+ in the roots. Compared

with the control, there was a greater increase in the halophyte. There was no difference between the two lines in the contents of K^+ in the root, which were reduced and showed an opposite trend to the Na^+. The subsequent transport by the stem contributed to the accumulation of Na^+ in the leaves. In the control, the contents of K^+ and the K^+/Na^+ ratio of the roots, stems, and leaves of the halophyte were higher than those of the non-halophyte. The K^+/Na^+ ratios of the roots, stems, and leaves of the two lines decreased significantly after the salt treatment, but those of the stems and leaves of the halophyte were higher than those of the non-halophyte. Under salt stress, there was a higher content of K^+ in the halophyte leaves, while there were lower contents of Na^+ in the stems and leaves (Fig. 7a-c).

Salt stress also enhanced the accumulation of N in both the roots and leaves. There were significantly higher concentrations of N in the roots and leaves of the halophyte than in the non-halophyte when exposed to salt. Compared with the control, the concentration of N in the halophyte increased by 46% in the roots and 28.9% in the leaves, while those of the non-halophyte increased by 49.1% and 28%, respectively. The concentration of P in the stems and leaves also increased after salt treatment. The concentration of P in the stems of the halophyte increased by 69.2%, and that of the non-halophyte increased by 40.7%. In terms of total content, the concentrations of P in the stems and leaves of the halophyte were 40.7% and 57.23% higher than those of the non-saline line, respectively, and the difference was significant. After the salt treatment, the N/P ratio in the roots and leaves of both lines decreased slightly, while that in the stems increased. Compared with the non-halophyte, the N/P ratio in the halophyte varied more, indicating that the halophyte is more sensitive to salt stress (Fig. 7d–f).

Discussion

In most cases, alien species tend to select habitats that resemble their native environments for invasion and colonization (Dietz and Edwards 2006; Vanet al. 2011). Interestingly, as a species that is generally considered to be a non-halophyte, we found that *I. cairica* could invade the saline environment. In our study, by comparing the responses of the halophyte line and the non-halophyte line of *I. cairica* to salt stress, it was shown that the halophyte *I. cairica* has obtained salt tolerance. To our knowledge, this is the first observation of salt tolerance in this species.

Morphological changes in the two lines under salt stress

Salt tolerance in plants is related to various aspects of plant physiology, biochemistry, morphology, and molecular mechanisms, which are all related to osmosis, photosynthesis, and nutrient imbalances that limit plant growth through salt stress and reduce the biomass of all parts of the plant (Flowers and Colmer 2008; Rahneshan et al. 2018; Chourasia et al. 2022). Our results indicated that the halophyte line is more capable of growing in saline habitats compared with the non-halophyte line. The stems of the halophyte appeared to regenerate more strongly, suggesting that they were more effective at reproducing asexually; this may play a key role in its invasion in saline habitats (Hu et al. 2014; Wang et al. 2017). The decrease in the number of branches and the advance of the flowering period indicate that the halophyte

allocates more energy to stem growth and sexual reproduction for both escape and adaptation (Amasino 2010; Liu et al. 2011).

Effects of salt stress on the chlorophyll content and fluorescence properties

Chlorophyll fluorescence parameters are often used to examine the relationship between the photosynthesis of plants and the environment in which they live and are important indicators that reflect the physiology of photosynthesis (Zhao et al. 2021; Ran et al. 2022). The Fv/Fm indicates the level of photoinhibition (Athar et al. 2005). In this study, the Fv/Fm remained stable across both lines under both treatments, which indicated that there was little photoinhibition; this suggests that both lines can adapt photosynthetically to salt stress (Ehsen et al. 2019; Bano et al. 2022). The sharper reduction in the Y(II), qL, and ETR of the non-halophyte line under NaCl treatment indicates that its PSII reaction center is more susceptible to damage and inactivated to a greater extent than that of the halophyte. We also observed a greater increase in NPQ in the non-halophyte under salt treatment, which protected the photosynthetic apparatus from damage by dissipating excess light energy in the form of heat through non-photochemical processes (Wei et al. 2006; Moinuddin et al.2017; Abideen et al. 2022). Salt stress may disrupt the biochemistry of photosynthesis, which decreases the efficiency of PSI and PSII owing to disturbances in the integrity of chloroplasts (Ibrahim et al. 2015; Stadnik et al. 2022). Therefore, it can be suggested that the halophyte is more tolerant to salinity stress owing to its ability to maintain the contents of chlorophyll and its fluorescence parameters.

Indicators of oxidative stress and cell damage under salt stress

Cells of the halophyte entered the apoptotic stage later than those of the non-halophyte, which indicates that the halophyte is better at maintaining photosynthesis and cell homeostasis in the saline environment (Katsuhara et al. 1996; Ameisen 2002). MDA is an important indicator of tolerance to salinity, which increases the degree of oxidative damage to the membrane (Koca et al. 2007; Ahmad et al. 2015; Feki et al. 2018). The REC represents the degree of damage to the plant cell membrane under stress (Esfandiari et al. 2020; Zhu et al. 2021). The halophyte showed a lower degree of cell membrane lipid peroxidation and a lower increase in the levels of REC and MDA, which indicate that the halophyte is more effective at maintaining the stability of the cell membrane structure and reducing the oxidative damage to the cells under salt stress than the non-halophyte. The integrity of the cell membrane of the halophyte was also higher than that of the non-halophyte, which is also consistent with the characteristics of salt-tolerant plants (Hasegawa et al. 2000).

Salt stress response of the antioxidant capacity and osmotic defenses

Under salt treatment, the lower degree of cell damage of the halophyte was associated with a higher antioxidant capacity. The accumulation of Pro is an important adaptive strategy under salt stress that contributes to the increase in salt tolerance (Slama et al. 2015; Martinez et al. 2016; Shirazi et al. 2018). Anthocyanins are natural pigments that protect antioxidant enzymes, scavenge free radicals, regulate cellular osmotic pressure, and stabilize the photosynthetic structure, thus, limiting the inhibition of plant

growth (Oswin and Kathiresan 1994; Zeng et al. 2010; Sun et al. 2017; Wang et al. 2019; Naing and Kim 2021; Zhao et al. 2023). Antioxidant enzymes are another method that plants can use to scavenge reactive oxygen species and resist oxidative damage, and they include SOD, POD, and CAT (Gaber 2010; Gill and Tuteja 2010; Wu et al. 2020; Yang et al. 2020; Ji et al. 2022). In this study, both halophyte and non-halophyte lines enhanced their antioxidant capacity by increasing the activities of POD, SOD, and CAT under salt stress. The molecular regulation of the activities of POD and SOD in salt-tolerant plants increased significantly under salt treatment to maintain the balance of metabolism of reactive oxygen species, which could be related to the high level of expression of IcSRO1 (Yuan et al. 2020).

Effects of salt stress on the stomata and salt glands

Both halophytes and non-halophytes improve their water use efficiency by reducing the number and density of stomata under salt stress (Tao et al. 2021). The halophyte line reduced the density of stomata, decreased their number, and reduced the rate of water loss to improve the tolerance to salt and preserve the water potential in cells under osmotic stress conditions (Munns et al. 2019, 2020; Zhao et al. 2021). This is also supported by findings in wheat (Triticum aestivum) (Tao et al. 2021), barley (Hordeum vulgare) (Kiani-Pouya et al. 2020), and species of cordgrass (Spartina spp.) (Maricle et al. 2009). These observations emphasize the importance of reducing the stomatal density as a strategy to escape the stress of saline conditions.

Salt glands play a pivotal role in the secretion of salt in recretohalophytes that secrete excess Na^+ to prevent damage from salt (Yuan and Wang 2020). The halophyte appeared to have more salt glands, a higher density and a larger area of them, which enables the halophyte to secrete excess salt through the salt glands to adapt to saline environments (Yuan et al. 2019; Wei et al. 2020; Yuan et al. 2022; Zhao et al. 2023).

Nutrient management

Salt stress disturbs the ionic balance of cells and activates the ion channels in the cell membranes, which causes an efflux of K^+ (Shabala et al. 2006; Kaydan et al. 2007). Therefore, maintaining high levels of K^+ and ensuring that the Na^+ in cytoplasm remains low is a common strategy to facilitate the proper function of enzymes and metabolic activities (Zhang et al. 2018). The halophyte line exhibits its advantages in terms of element balance by maintaining a high K^+/Na^+ ratio, which is necessary to maintain enzymatic activity and is even more important than keeping the levels of Na^+ low (Sun et al. 2019; Fang et al. 2021; Hongna et al. 2021). With a higher K^+/Na^+ ratio than the non-halophyte line, the halophyte obtained a more balanced ion content and more stable growth (Rahman et al. 2016; Wu et al. 2021; Zhang et al. 2023). Moreover, the halophyte transports large amounts of salt ions into its stems and leaves, thereby reducing the negative impacts of excessive ions on the root system (Qin et al. 2018). These findings have led to suggestions to improve salt tolerance by removing Na^+ from the stems and leaves, providing K^+ to the stems, and retaining K^+ in the leaf tissue to maintain an optimal K^+/Na^+ ratio in the stems and leaves.

The accumulation of N, P and K^+ in the leaves promotes plant growth and development (Wang et al. 2021), while the maintenance of the K^+/Na^+ ratio and N/P ratio in leaves; the selective transport of K^+, N and P from the roots to leaves; and the accumulation of Pro in the leaves helps to reduce the toxic effects of Na^+ and the damage caused by osmotic stress (Zelm et al. 2020; Pan et al. 2022). After acclimatization to the salt environment, the halophyte line allocated more nutrient resources to the leaves to construct morphogenesis and ultimately enhance photosynthesis (Jayaraman et al. 2002; Niemi et al. 2004; Osman et al. 2018). Phosphorus is also related to the structural composition and protein activity of plants (Ratnayake et al. 1978). The accumulation of P may improve the integrity of the leaf cells in the halophyte, thereby accelerating the biosynthesis of photosynthetic products.

Conclusions

In this study, we investigated the growth, physiological, and biochemical responses of two lines against salt stress. According to the results, salt stress is reflected in the obvious impairment of photosynthetic performance and the inhibition of Y(II), NPQ, ETR, and chlorophyll biosynthesis. An increase in the concentration of MDA and REC highlighted the lipid peroxidation and oxidative damage to cell membranes. However, the adverse effects of salt stress could be mitigated by various internal mechanisms in the cell, such as the accumulation of antioxidant enzymes (SOD, POD, and CAT) and osmolytes (Pro and anthocyanins) (Fig. 8). The halophyte of *I. cairica* in Zhuhai and the non-halophyte in Guangzhou appeared to have different physiological responses to salt stress. The halophyte line was considerably less inhibited, which demonstrates that it has rapidly adjusted to increase its adaptability to salt and enhance its invasiveness in mangrove wetland ecosystems. In addition, this adaptability might be heritable, and it will be investigated further in our subsequent research.

Declarations

Acknowledgments We thank Professor Paul Giller from the School of Biological, Earth and Environmental Sciences, University College of Cork, Ireland for the English language editing.

Author contributions TTX and MHC conceived and designed research. JTZ and BQY conducted the experiments. TTX, WHL, and XTX supervised project administration. JTZ and MHC wrote the manuscript. TTX and JTZ revised the manuscript. All authors read and approved the manuscript.

Funding This research was funded by the National Natural Science Foundation of China (grant no. 32071618), and Natural Science Foundation of Guangdong Province (grant no. 2023A1515012608).

Data availability The data that support the findings of this study are available from the corresponding author upon reasonable requests.

Confict of interest The authors declare that they have no known competing financial interests or personal relationships that could have appeared to influence the work reported in this paper.

References

1. Abideen Z, Koyro HW, Hussain T, Rasheed A, Alwahibi MS, Elshikh MS, Hussain MI, Zulfiqar F, Mansoor S, Abbas Z (2022) Biomass Production and Predicted Ethanol Yield Are Linked with Optimum Photosynthesis in *Phragmites karka* under Salinity and Drought Conditions. Plants 11: 1657. https://doi.org/10.3390/plants11131657.
2. Acosta-Motos JR, Diaz-Vivancos P, Alvarez S, Fernandez-Garcia N, Sanchez-Blanco MJ, Hernandez JA (2015) NaCl-induced physiological and biochemical adaptative mechanisms in the ornamental *Myrtus communis* plants. J. Plant Physiol. 183: 41–51.
3. Aebi H (1984) Catalase in vitro. In Methods in Enzymology; Academic Press: New York, NY, USA
4. : 121–126. ISBN 0076-6879.
5. Ahmad P, Azooz MM, Prasad MNV (2013) Ecophysiology and Responses of Plants under Salt Stress; Springer: New York, NY, USA; Heidelberg, Germany; Dordrecht, The Netherlands; London, UK.
6. Ahmad P, Hashem A, Abd-Allah EF, Alqarawi AA, John R, Egamberdieva D, Gucel S (2015) Role of Trichoderma harzianum in mitigating NaCl stress in Indian mustard (*Brassica juncea*) through antioxidative defense system. Front. Plant Sci 6: 868.
7. Allakhverdiev SI (2020) Optimising photosynthesis for environmental fitness. Funct Plant Biol 47: iii-vii.
8. Almeida DM, Oliveira MM, Saibo NJM (2017) Regulation of Na^+ and K^+ homeostasis in plants: towards improved salt stress tolerance in crop plants. Genet Mol Biol 40: 326–345.
9. Alzahrani SM, Alaraidh IA, Migdadi H, Alghamdi S, Altaf Khan M, and Ahmad P (2019) Physiological, biochemical, and antioxidant properties of two genotypes of *Vicia faba* grown under salinity stress. Pak. J. Bot. 51: 786–798. Doi:10.30848/PJB2019-3(3)
10. Amasino R (2010) Seasonal and developmental timing of flowering. Plant J 61(6): 10011013.
11. Ameisen J (2002) On the origin, evolution, and nature of programmed cell death: a timeline of four billion years. Cell Death Differ 9(4): 367-393.
12. Athar HuR, Ashraf M (2005) Photosynthesis under Drought Stress. In Handbook of Photosynthesis, 2nd ed.; Pessarakli, M., Ed.; CRCPress: Boca Raton, FL, USA, pp. 793–809.
13. Bai F, Chisholm R, Sang W, Dong M (2013) Spatial risk assessment of alien invasive plants in China. Environ Sci Technol 47:7624–7632.
14. Baker NR (2008) Chlorophyll fluorescence: A probe of photosynthesis in vivo. Annu. Rev. Plant Biol. 59: 89–113.
15. Baker NR, Rosenqvist E (2004) Applications of chlorophyll fluorescence can improve crop production strategies: An examination of future possibilities. J. Exp. Bot. 55: 1607–1621.
16. Bano S, Ahmed MZ, Abideen Z, Qasim M, Gul B, Khan NU (2022) Humic acid overcomes salinity barriers and stimulates growth of *Urochondra setulosa* by altering ion-flux and photochemistry. Acta Physiol. Plant 44: 39.

17. Barbieri G, Vallone S, Orsini F, Paradiso R, De Pascale S, Negre-Zakharov F, Maggio A (2012) Stomatal density and metabolic determinants mediate salt stress adaptation and water use efficiency in basil (*Ocimum basilicum*). J. Plant Physiol. 169: 1737–1746.
18. Bellard C, Cassey P, Blackburn TM (2016) Alien species as a driver of recent extinctions. Biol. Lett. 12 (2), 20150623. https://doi.org/10.1098/rsbl.2015.0623.
19. Biswas S, Choudhury J, Nishat A, Rahman M (2007) Do invasive plants threaten the Sundarbans mangrove forest of Bangladesh? Forest Ecology and Management 245(1-3): 1-9.
20. Blum A (2017) Osmotic adjustment is a prime drought stress adaptive engine in support of plant production. Plant Cell Environ. 40 (1): 4-10. https://doi.org/10.1111/pce.12800.
21. Bouchereau A, Flowers T, Savoure A (2015) Diversity, distribution and roles of osmoprotective compounds accumulated in halophytes under abiotic stress. Ann. Bot. 115: 433–447.
22. Cao WH, Liu J, He XJ, Mu RL, Zhou HL, Chen SY, Zhang JS (2007) Modulation of ethylene responses affects plant salt-stress responses. Plant Physiol. 143: 707–719.
23. Chen M, Xu SQ (2007) The role of mangroves in coastal ecosystems [J]. Success (Education), (04):87-88.
24. Chen M, Cai M, Xiang P, Qin Z, Peng C, Li S (2022) Thermal adaptation of photosynthetic physiology of the invasive vine *Ipomoea cairica (L.)* enhances its advantage over native Paederia scandens (Lour.) Merr. in South China [J]. Tree Physiology. tpac139.
25. https://doi.org/10.1093/treephys/tpac139
26. Chourasia KN, More SJ, Kumar A (2022) Salinity responses and tolerance mechanisms in underground vegetable crops: an integrative review. Planta. 255: 68. https://doi.org/10.1007/s00425-022-03845-y
27. Dietz H, Edwards P (2006) Recognition that causal processes change during plant invasion helps explain conflicts in evidence. Ecology 87(6): 1359-1367.
28. Ding F, Chen M, Sui N, Wang BS (2010) Ca^{2+} significantly enhanced development and salt-secretion rate of salt glands of Limonium bicolor under NaCl treatment. South African Journal of Botany 76(1): 95–101. https://doi.org/10.1016/j.sajb.2009.09.001
29. Ding H, Xu HG, Wu J (2009) Status and trends of invasive alien species in China. World Environment. (3): 39-40.
30. Dong XY, Fu J, Yin XB, Qu CH, Yang CJ, Li HY, He GQ, Ni J (2017) Induction of Apoptosis in HepaRG Cell Line by Aloe-Emodin through Generation of Reactive Oxygen Species and the Mitochondrial Pathway. Cellular Physiology and Biochemistry. 42(2): 685–696.
31. Ehsen S, Abideen Z, Rizvi RF, Gulzar S, Aziz I, Gul B, Khan MA, Ansari R (2019) Ecophysiological adaptations and anti-nutritive status of sustainable cattle feed Haloxylon stocksii under saline conditions. Flora 257: 151425.
32. Esfandiari Ghalati R, Shamili M, Homaei A (2020) Effect of putrescine on biochemical and physiological characteristics of guava (*Psidium guajava*) seedlings under salt stress. Sci. Hortic.

261: 108961.
33. Fan S, Wu H, Gong H, Guo J (2022) The salicylic acid mediates selenium-induced tolerance to drought stress in tomato plants. Sci Hortic 300: 111092. https://doi.org/10.1016/j.scienta.2022.111092
34. Fang S, Hou X, Liang X (2021) Response mechanisms of plants under saline-alkali stress. Front Plant Sci 12: 667458.
35. Feki K, Tounsi S, Brini F (2018) Comparison of an antioxidant system in tolerant and susceptible wheat seedlings in response to salt stress. Span. J. Agric. Res. 15: 0805.
36. Flowers TJ, Colmer TD (2008) Salinity tolerance in halophytes [J]. New Phytologist 179(4): 945-963.
37. Fu XC, Chen YJ, HB, Lei J, Yang HB, Wen J, Du PQ, Jiang ZG (2022) Soil properties and their differences in Guangtan, Spartina alterniflora community area and artificial mangrove forest area of Qiao Island [J]. Wetland Science, 20(05):715-720.
38. Gaber M Abogadallah (2010) Antioxidative defense under salt stress. Plant Signal Behav 5(4): 369-74.
39. Galbraith D, Harkins K, Maddox J, Ayres N, Sharma D, Firoozabady E (1983) Rapid flow cytometric
40. analysis of the cell cycle in intact plant tissues[J]. Science. 220(4601): 1049-1051.
41. Ge BM, Bao YX, Cheng HY, Zhang DZ, Hu ZY (2012) Influence of Spartina alterniflora invasion stages on macrobenthic communities on a tidal flat in Wenzhou Bay, China. Braz. J. Oceanogr. 60: 441–448.
42. Genc Y, Oldach K, Taylor J, Lyons GH (2016) Uncoupling of sodium and chloride to assist breeding for salinity tolerance in crops. New Phytol. 210: 145–156. doi:10.1111/nph.13757
43. Gould KS (2004) Nature's Swiss Army Knife: the diverse protective roles of anthocyanins in leaves. J Biomed Biotechnol 5:314–320.
44. Gu ZY, Wu XH, Yang G, Chen JD (2006) Status and Countermeasures against Invasion of Exotic Organisms in China. Jiangsu Agricultural Science. (6): 418-421.
45. Guan B, Yu J, Lu Z, Zhang Y, Wang X (2011) Effects of Water-Salt Stress on Seedling Growth and Activities of Antioxidative Enzyme of Suaeda Salsa in Coastal Wetlands of the Yellow River Delta. Environ. Sci. 32: 2422–2429.
46. Hao S, Wang Y, Yan Y, Liu Y, Wang J, Chen S (2021) A review on plant responses to salt stress and their mechanisms of salt resistance. Horticulturae 7: 132.
47. Hasanuzzaman M, Zhou M, Shabala S (2023) How Does Stomatal Density and Residual Transpiration Contribute to Osmotic Stress Tolerance? Plants 12: 494. https://doi.org/10.3390/plants12030494
48. Hasegawa P, Bressan R, Zhu J, Bohnert H (2000) Plant cellular and molecular responses to high salinity. Annu Rev Plant Phys 51(1): 463-499.
49. Hessini K, Issaoui K, Ferchichi S, Saif T, Abdelly C, Siddique K.H.M, Cruz C (2019) Interactive effects of salinity and nitrogen forms on plant growth, photosynthesis and osmotic adjustment in maize.

Plant Physiol. Biochem. 139: 171-179. https://doi.org/10.1016/j.plaphy.2019.03.005.

50. Hoagland D, Arnon D (1950) The water-culture method for growing plants without soil. Berkeley, University of California, pp 13-57.
51. Hoch W, Singsaas E, Mccown B (2003) Anthocyanins facilitate nutrient recovery in autumn by shielding leaves from potentially damaging light levels. Plant Physiol 133(3): 12961305.
52. Hongna C, Leyuan T, Junmei S, Xiaori H, Xianguo C (2021) Exogenous salicylic acid signal reveals an osmotic regulatory role in priming the seed germination of *Leymus* chinensis under salt-alkali stress. Environ Exp Bot 188:104498.
53. Hou YP, Peng SL, Lin ZG, Huang QQ, Ni GY, & Zhao N (2014) Fast-growing and poorly shade-tolerant invasive species may exhibit higher physiological but not morphological plasticity compared with non-invasive species. Biological Invasions. 17(5): 1555–1567. doi:10.1007/s10530-014-0815-x
54. Hu L, Li M, Wei P (2014) Salt tolerance of the invasive vine *Mikania micrantha* Ecology and Environmental Sciences 23(1): 7-15.
55. Huang QQ, Wu JM, Bai YY, Zhou L, Wang GX (2008) Identifying the most noxious invasive plants in China: Role of geographical origin, life form and means of introduction. Biodivers. Conserv. 2008, 18: 305–316.
56. Ibrahim W, Ahmed IM, Chen X, Cao F, Zhu S, Wu F (2015) Genotypic differences in photosynthetic performance, antioxidant capacity, ultrastructure and nutrients in response to combined stress of salinity and Cd in cotton. BioMetals 28: 1063–1078.
57. Jackson J, Kirby M, Berger W, Bjorndal K, Botsford L, Bourque B, Bradbury R, Cooke R, Erlandson J, Estes J (2001) Historical overfishing and the recent collapse of coastal ecosystems. Science 2001, 293(5530): 629-637.
58. Jayaraman A, Yang R, Cho S, Bhat T, Choudary V (2002) Adsorption of nitrogen, oxygen and argon on Na-CeX zeolites. Adsorption 8(4): 271-278.
59. Ji X, Tang J, Fan W, Li B, Bai Y, He J, Pei D, Zhang J (2022) Phenotypic Differences and Physiological Responses of Salt Resistance of Walnut with Four Rootstock Types. Plants 11: 1557. https://doi.org/10.3390/plants11121557
60. Jiang K, Chen X, Bao Y, Haihong LI, Shi W, Wang H (2016) Effect of Spartina alterniflora invasion on the vertical structure of macrobenthic community. Acta Ecol. Sin. 36(2): 535–544.
61. Kao K, Michayluk M (1974) A method for high-frequency intergeneric fusion of plant protoplasts. Planta 115(4): 355-367.
62. Katsuhara M, Kawasaki T (1996) Salt Stress Induced Nuclear and DNA Degradation in Meristematic Cells of Barley Roots. Plant and Cell Physiology 37(2): 169–173. https://doi.org/10.1093/oxfordjournals.pcp.a028928
63. Kaydan D, Yagmur M, Okut NJ (2007) Effects of salicylic acid on the growth and some physiological characters in salt stressed wheat (*Triticum aestivum*). Tarim Bilimleri Dergisi 13(2): 11-119.

64. Kiani-Pouya A, Rasouli F, Rabbi B, Falakboland Z, Yong M, Chen, ZH (2020) Stomatal traits as a determinant of superior salinity tolerance in wild barley. J. Plant Physiol. 245: 153108. Doi: 10.1016/j.jplph.2019.153108
65. Koca H, Melike B, Özdemir F, Türkan I (2007) The effect of salt stress on lipid peroxidation, antioxidative enzymes and proline content of sesame cultivars. Environ. Exp. Bot. 60: 344–351.
66. Lawlor DW (1995) Photosynthesis, productivity and environment. J Exp Bot 46:1449–1461.
67. Leng BY, Yuan F, Dong XX, Wang J, & Wang BS (2018) Distribution pattern and salt excretion rate of salt glands in two recretohalophyte species of *Limonium* (Plumbaginaceae). South African Journal of Botany 115: 74–80. https://doi.org/10.1016/j.sajb.2018.01.002
68. Lequeux H, Hermans C, Lutts S, Verbruggen N (2010) Response to copper excess in *Arabidopsis thaliana*: impact on the root system architecture, hormone distribution, lignin accumulation and mineral profile. Plant PhysiolBioch 48(8): 673-682.
69. Lin P (1997) Mangrove Ecosystem in China. Beijing, Science Press pp 1997: 14-59.
70. Liu G, Huang QQ, Lin ZG, Huang FF, Liao HX, Peng SL (2012) High tolerance to salinity and herbivory stresses may explain the expansion of *Ipomoea cairica* to salt marshes. PLoS One 7: e48829.
71. Liu G, Guan R, Chang R, Qiu L (2011) Correlation between Na^+ Contents in Different Organs of Soybean and Salt Tolerance at the Seedling Stage. Acta Agronomica Sinica 37(7): 1266-1273.
72. Luo B, Wang C, Wang XD, Zhang H, Zhou YN, Wang WS (2021) Changes in photosynthesis and chlorophyll fluorescence in two soybean (Glycine max) varieties under NaCl stress. Int J Agric & Biol Eng 14(3): 76–82.
73. Martinez V, Mestre TC, Rubio F, Girones-Vilaplana A, Moreno DA, Mittler R, Rivero RM (2016) Accumulation of flavonols over hydroxycinnamic acids favors oxidative damage protection under abiotic stress. Front. Plant Sci. 7: 838.
74. Moinuddin M, Gulzar S, Hameed A, Gul B, Ajmal Khan M, Edwards GE (2017) Differences in photosynthetic syndromes of four halophytic marsh grasses in Pakistan. Photosynth. Res. 131: 51–64.
75. Morimaru K, Mitsutoshi T, Yasuo I, Kazutoshi K, Toshiyuki O, Nobuhide F (2017) High salinity leads to accumulation of soil organic carbon in mangrove soil. Chemosphere 177:51-55. https://doi.org/10.1016/j.chemosphere.2017.02.074
76. Munns R, Day DA, Fricke W, Watt M, Arsova B, Barkla BJ, (2019) Energy costs of salt tolerance in crop plants. New Phytol. 225: 1072–1090. Doi: 10.1111/nph.15864
77. Munns R, Passioura JB, Colmer TD, Byrt CS (2020) Osmotic adjustment and energy limitations to plant growth in saline soil. New Phytol 225: 1091–1096. Doi: 10.1111/nph.15862
78. Naing AH, Kim CK (2021) Abiotic stress-induced anthocyanins in plants: their role in tolerance to abiotic stresses. Physiol Plant 172:1711–1723.
79. Naing AH, Park KI, Ai TN, Chung MY, Han JS, Kang YW et al (2017) Overexpression of snapdragon Delila (Del) gene in tobacco enhances anthocyanin accumulation and abiotic stress tolerance. BMC

Plant Biol 17:65.

80. Naz N, Fatima S, Hameed M (2022) Modulation in Plant Micro-structures Through Soil Physicochemical Properties Determines Survival of *Salsola imbricata* in Hypersaline Environments. J Soil Sci Plant Nutr 22: 861–881. https://doi.org/10.1007/s42729-021-00697-5
81. Niemi G, Wardrop D, Brooks R, Anderson S, Brady V, Paerl H, Rakocinski C, Brouwer M, Levinson B, McDonald M (2004) Rationale for a new generation of indicators for coastal waters. Environ Health Persp 112(9): 979-986.
82. Orsini F, Alnayef M, Bona S, Maggio A, Gianquinto G (2012) Low stomatal density and reduced transpiration facilitate strawberry adaptation to salinity. Environ. Exp. Bot. 81: 1–10.
83. Osman KT (2018) Saline and Sodic Soils. In *Management of Soil Problems*; Springer International Publishing AG, Part of Springer Nature: Cham, Switzerland, 2018; pp. 255–293.
84. Oswin S, Kathiresan K (1994) Pigments in mangrove species of Pichavaram. Indian J Geo-Mar Sci 23(1): 64-66.
85. Pan J, Xue X, Huang C, Peng F, Liao J, Ma S, You Q, Wang T (2022) Salt Tolerance Strategies of *Nitraria tangutorum* And *Elaeagnus angustifolia* Linn. Determine the Inoculation Effects of Microorganisms in Saline Soil Conditions. Agronomy 12: 913. https://doi.org/10.3390/agronomy12040913
86. Qin Y, Bai J, Wang Y, Liu J, Hu Y, Dong Z, Ji L (2018) Comparative effects of salt and alkali stress on photosynthesis and root physiology of oat at anthesis. Arch Biol Sci 70(2): 329-338.
87. Quan W, Zhang H, Wu Z, Jin S, Tang F, Dong J (2016) Does invasion of Spartina alterniflora alter microhabitats and benthic communities of salt marshes in Yangtze River estuary? Ecol. Eng. 88: 153–164.
88. Rahman A, Nahar K, Hasanuzzaman M, Fujita M (2016) Calcium Supplementation Improves Na (+)/K (+) Ratio, Antioxidant Defense and Glyoxalase Systems in Salt-Stressed Rice Seedlings. Front Plant Sci 7: 609. Doi:10.3389/fpls.2016.00609
89. Ran X, Wang X, Huang X, Ma C, Liang H and Liu B (2022) Study on the Relationship of Ions (Na, K, Ca) Absorption and Distribution to Photosynthetic Response of *Salix matsudana* Koidz Under Salt Stress. Front. Plant Sci. 13: 860111. Doi: 10.3389/fpls.2022.860111
90. Ratnayake M, Leonard R, Menge J (1978) Root exudation in relation to supply of phosphorus and its possible relevance to mycorrhizal formation. New Phytol 81(3): 543-552.
91. Ren H, Guo Q, Liu H, Li J, Zhang Q, Xu H, Xu F (2014) Patterns of alien plant invasion across coastal bay areas in southern China. J Coastal Res 295: 448-455.
92. Shabala S, Demidchik V, Shabala L, Cuin T, Smith S, Miller A, Davies J, Newman I (2006) Extracellular Ca^{2+} ameliorates NaCl-induced K^+ loss from Arabidopsis root and leaf cells by controlling plasma membrane K^+ -permeable channels. Plant Physiol 141(4): 1653-1665.
93. Shen XY, Peng SL, Chen BM, et al. (2011) Do higher resource capture ability and utilization efficiency facilitate the successful invasion of native plants [J]. Biological Invasions. 13(4): 869-881.

94. Shi Y, Zhang Y, Han W, Feng R, Hu Y, Guo J, Gong H (2016) Silicon enhances water stress tolerance by improving root hydraulic conductance in *Solanum lycopersicum* Front Plant Sci 7: 196. https://doi. org/ 10. 3389/fpls.2016. 00196
95. Shirazi M, Khan M, Mahboob W, Khan MA, Shereen A, Mujtaba S, Asad A (2018) Inconsistency in salt tolerance of some wheat (*Triticum aestivium*) genotypes evaluated under various growing environments. Pak. J. Bot. 50: 471–479.
96. Slingsby JA, Merow C, Aiello-Lammens M, Allsopp N, Hall S, Kilroy Mollmann H, Turner R, Wilson AM, Silander JA (2017) Intensifying postfire weather and biological invasion drive species loss in a Mediterranean-type biodiversity hotspot. PNAS. 114 (18): 4697–4702. https://doi.org/10.1073/pnas.1619014114.
97. Smith VR (1979) A comparison between the H_2SO_4-H_2O_2-Li_2SO_4-Se oxidation method and alternative digestion procedures for plant nutrient analysis. Commun Soil Sci Plan 10(7): 1067-1077.
98. Stadnik B, Tobiasz-Salach R, Mazurek M (2022) Physiological and Epigenetic Reaction of Barley (Hordeum vulgare L.) to the Foliar Application of Silicon under Soil Salinity Conditions. Int. J. Mol. Sci. 23: 1149. https://doi.org/10.3390/ijms23031149
99. Sun M, Feng XX, Gao JJ, Peng RH, Yao QH, Wang LJ (2017) VvMYBA6 in the promotion of anthocyanin biosynthesis and salt tolerance in transgenic Arabidopsis. Plant Biotechnol Rep 11: 299–314.
100. Tao R, Ding J, Li C, Zhu X, Guo W, Zhu M (2021) Evaluating and Screening of Agro-Physiological Indices for Salinity Stress Tolerance in Wheat at the Seedling Stage. Front. Plant Sci. 12: 646175. Doi: 10.3389/fpls.2021.646175
101. Tognon GB, Petry C, Cuquel FL (2012) RESPONSE TO WATER DEFICIT OF Ipomoea cairica (L.) SWEET. CIENCIA E AGROTECNOLOGIA 36 (3). https://doi.org/10.1590/S1413-70542012000300007
102. Van Kleunen M, Schlaepfer D, Glaettli M, Fischer M (2011) Preadapted for invasiveness: do species traits or their plastic response to shading differ between invasive and non-invasive plant species in their native range? J Biogeogr 38(7): 1294-1304.
103. Wang C, Lu G, Hao Y, Guo H, Guo Y, Zhao J, Cheng H (2017) ABP9, a maize bZIP transcription factor, enhances tolerance to salt and drought in transgenic cotton. Planta 246: 453–469.
104. Wang CW and others (2022) Photosynthesis in response to salinity and submergence in two Rhizophoraceae mangroves adapted to different tidal elevations. Tree Physiology 42(5): 1016–1028. https://doi.org/10.1093/treephys/tpab167
105. Wang F, Ren X, Zhang F, Qi M, Zhao H, Chen X (2019) A R2R3-type MYB transcription factor gene from soybean, *GmMYB12*, is involved in flavonoids accumulation and abiotic stress tolerance in transgenic Arabidopsis. Plant Biotechnol Rep 13: 219–233.
106. Wang J, Jiang M, Nie Z (2022) ABA participates in salt stress-induced anthocyanin accumulation by stimulating the expression of *LrMYB1* in *Lycium ruthenicum Murr*. Plant Cell Tiss Organ Cult 151: 11–21. https://doi.org/10.1007/s11240-022-02325-1

107. Wang R, Wang C, Feng Q, Liou RM, Lin YF (2021) Biological inoculant of salt-tolerant bacteria for plant growth stimulation under different saline soil conditions. J Microbiol Biotechnol 31: 398–407.
108. Wang RL, Zeng RS, Peng SL et al. (2011) Elevated temperature may accelerate invasive expansion of the liana plant *Ipomoea cairica* [J]. Weed Research. 51(6): 574-580.
109. Wang Y, Muller-Scharer H, van Kleunen M, Cai A, Zhang P, Yan R, Dong B, Yu F (2017) Invasive alien plants benefit more from clonal integration in heterogeneous environments than natives. New Phytol 216(4): 1072-1078.
110. Wei L, Zhang J, Wei S, Hu D, Liu Y, Feng L, Li C, Qi N, Wang C, Liao W (2022) Nitric Oxide Enhanced Salt Stress Tolerance in Tomato Seedlings, Involving Phytohormone Equilibrium and Photosynthesis. Int. J. Mol. Sci. 23: 4539. https://doi.org/10.3390/ijms23094539
111. Wei X, Yan X, Yang Z (2020) Salt glands of recretohalophyte *Tamarix* under salinity: Their evolution and adaptation. Ecol Evol. 10: 9384–9395. https://doi .org/10.1002/ece3.6625
112. Wei Y, Xu X, Tao H, Wang P (2006) Growth performance and physiological response in the halophyte *Lycium barbarum* grown at salt-affected soil. Ann. Appl. Biol. 149: 263–269.
113. Wu GQ, Li H, Zhu YH, Li SJ (2021) Comparative physiological response of sainfoin (*Onobrychis viciaefolia*) seedlings to alkaline and saline-alkaline stress. J Anim Plant Sci 31:1028–1035.
114. Wu YQ, Hu YJ (2004) Exotic plants wedelia, split leaf petunia and five claws Photosynthetic characteristics of Golden dragon [J]. Acta Ecologica Sinica. 24(10): 2334-2339.
115. Wu Z, Wang J, Yan D, Yuan H, Wang Y, He Y, Wang X, Li Z, Mei J, Hu M (2020) Exogenous spermidine improves salt tolerance of pecan-grafted seedlings via activating antioxidant system and inhibiting the enhancement of Na^+/K^+ Acta Physiol. Plant 42: 83.
116. Yang C, Xu H, Wang L, Liu J, Shi D, Wang D (2009) Comparative effects of salt-stress and alkali-stress on the growth, photosynthesis, solute accumulation, and ion balance of barley plants. Photosynthetica 47(1):79–86
117. Yang Z, Li JL, Liu LN (2020) Photosynthetic regulation under salt stress and salt-tolerance mechanism of sweet sorghum. Front. Plant Sci 10: 1722.
118. Yokoi S, Bressan RA, Hasegawa PM (2002) Salt stress tolerance of plants. JIRCAS Working Report. 25-33. Available: http://www.plantstress.com/articles/salinity_m/salinity_m_files/jircas.pdf.
119. Yu XH, Li SS (2019) Prevention and control of exotic invasive plants and prospects of their resource utilization [J]. Hunan Agricultural Sciences. 58(4): 5-8.
120. Yuan B, Chen M, Li S (2020) Isolation and identification of *Ipomoea cairica* (L.) Sweet gene *IcSRO1* encoding a SIMILAR TO RCD-ONE protein, which improves salt and drought tolerance in transgenic *Arabidopsis*. Int J Mol Sci 21(3): e1017.
121. Yuan F, Liang X, Li Y, Yin S, Wang B (2019) Methyl jasmonate improves salinity tolerance in Limonium bicolor by enhancing photosynthesis and abaxial salt gland density. Functional Plant Biology, 46(1), 82–92. https://doi.org/10.1071/FP18120

122. Yuan F, Wang B (2020) Adaptation of Recretohalophytes to Salinity. Handbook of Halophytes (Springer Cham), pp. 1–21.
123. Yuan F, Wang X, Zhao B, Xu X, Shi M, Leng B, Dong X, Lu C, Feng Z, Guo J, Han G, Zhang H, Huang J, Chen M, Wang BS (2022) The genome of the recretohalophyte *Limonium* bicolor provides insights into salt gland development and salinity adaptation during terrestrial evolution. Mol. Plant 15: 1024–1044.
124. Zelm EV, Zhang Y, Testerink C (2020) Salt Tolerance Mechanisms of Plants. Annual Review of Plant Biology 71(1): 403-433. https://doi.org/10.1146/annurev-arplant-050718-100005
125. Zeng X, Chow W, Su L, Peng X, Peng C (2010) Protective effect of supplemental anthocyanins on Arabidopsis leaves under high light. Physiol. Plant. 138(2): 215-225.
126. Zhao BQ, Zhou YL, Jiao XG, Wang X, Wang BS, Yuan F (2023) Bracelet salt glands of the recretohalophyte *Limonium* bicolor: Distribution, morphology, and induction. Journal of Integrative Plant Biology 65: 1672-9072. https://doi.org/10.1111/jipb.13417
127. Zhao J, Zhang W, da Silva JAT (2021) Rice histone deacetylase HDA704 positively regulates drought and salt tolerance by controlling stomatal aperture and density. Planta 254: 79. https://doi.org/10.1007/s00425-021-03729-7
128. Zhao R, Naing AH, Xu J (2023) Overexpression of anthocyanin regulatory transcription factors can alleviate salt stress-induced growth inhibition in torenia 'Kauai Rose'. Plant Biotechnol Rep 17: 203–212. https://doi.org/10.1007/s11816-023-00826-9
129. Zhao Y, Wu M, Deng P, Zhou XW, and Huang SY (2021) Effects of salt stress on growth and chlorophyll fluorescence parameters of *Siraitia grosvenorii* South China Fruits. 50: 103–107. Doi: 10.13938/j.issn.1007-1431.20200431
130. Zhang K, Chang L, Li G (2023) Advances and future research in ecological stoichiometry under saline-alkali stress. Environ Sci Pollut Res 30: 5475–5486.
131. Zhang Q, Huang J, Ke W, Cai M, Chen G, Peng C (2021) Responses of Sphagneticola trilobata, Sphagneticola calendulacea and their hybrid to drought stress. Int J Mol Sci 22:11288.
132. Zhang Y, Fang J, Wu X, Dong L (2018) Na^+/K^+ balance and transport regulatory mechanisms in weedy and cultivated rice (*Oryza sativa*) under salt stress. BMC Plant Biol. 18: 375. https://doi.org/10.1186/s12870-018-1586-9.
133. Zhang Z, Li J, Li Y, Liu WW, Chen YX, Zhang YH, Li YF (2021) Spatially discontinuous relationships between salt marsh invasion and mangrove forest fragmentation. Forest Ecology and Management. 499: 0378-1127. https://doi.org/10.1016/j.foreco.2021.119611
134. Zhu H, Ma RJ, Wu ST et al (2009) Effects of drought stress on seed germination and seedling growth of A. pentaphyllum [J]. Northwest Journal of Botany. 29(02): 344-349.
135. Zhu H, Shuangtao W (2012) Impacts of invasion of *Ipomoea cairica* on plant community and soil fertility. J Ecol Rural Environ 28:505–510.
136. Zhu J (2016) Abiotic stress signaling and responses in plants. Cell. 167(2): 313-324.

137. Zhu S, Nong J, Luo G, Li Q, Wang F, Jiang D, Zhao X (2021) Varied tolerance and different responses of five citrus rootstocks to acid stress by principle component analysis and orthogonal analysis. Sci. Hortic. 278: 0304-4238.

Figures

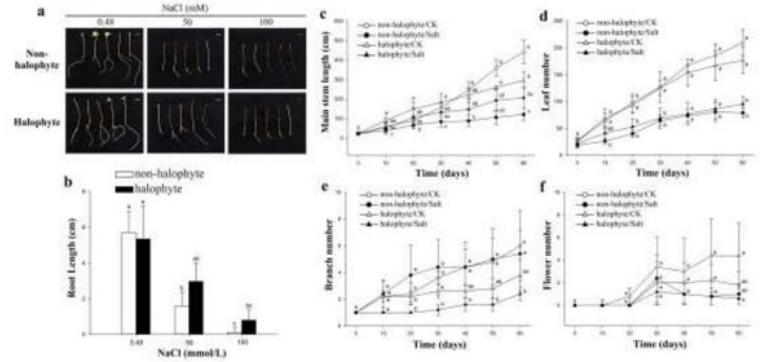

Fig. 1

Figure 1

The growth of different lines of *Ipomoea cairica* under salt stress that shows the phenotypic adaptability of the halophyte to salt stress. (**a**-**b)** Root growth after 2 weeks of hydroponics, including (**a)** The morphology of root, bar=1 cm. (**b)** Bar graph showing the root length. (**c**-**f)** The growth trend of the two lines within 60 d after transplanting, including. (**c)** The tendency of main stem to grow. (**d)** Leaf number during the salt treatment. (**e)** Branch number. (**f)** Flower number. All the data represent the mean ± SD. The different letters in the bar graphs indicate significant differences at $P < 0.05$. SD, standard deviation.

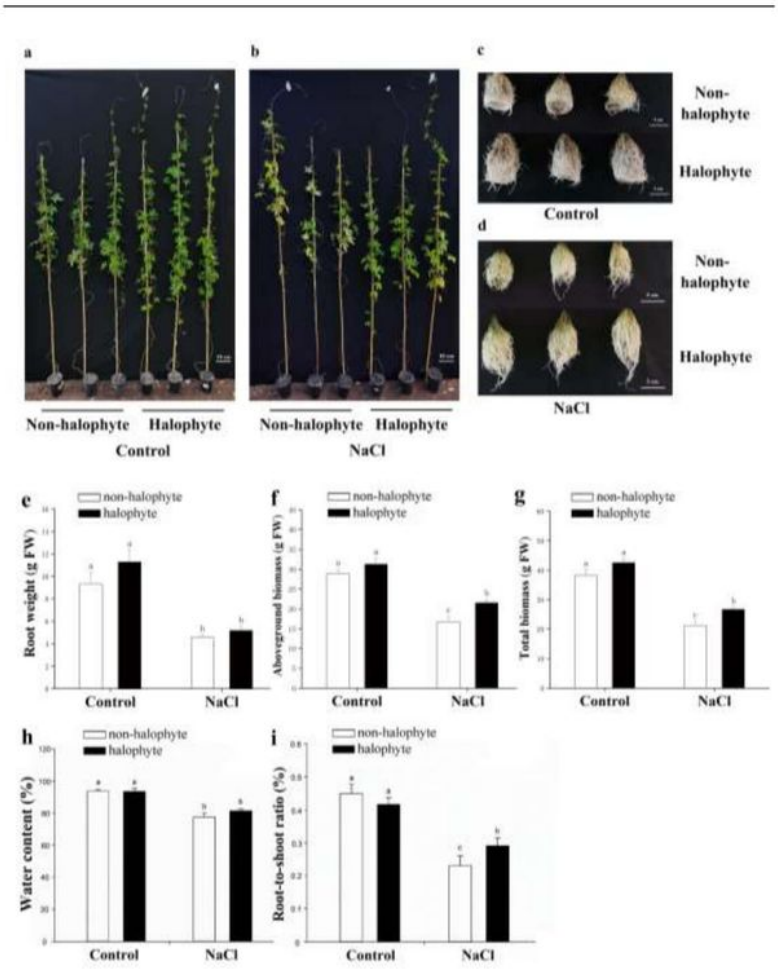

Fig. 2

Figure 2

Effect of 150 mmol/L NaCl on the growth of non-halophytic and halophytic lines of *Ipomoea cairica* **(a-d)** After 60 d. **(e)** Fresh weight of the roots. **(f)**Fresh weight of the aboveground biomass. **(g)** Fresh weight of the total biomass. **(h)** Water content. **(i)** Root-to-shoot ratio. All the data represent the mean ± SD. Different letters indicate a significant difference at $P < 0.05$. SD, standard deviation.

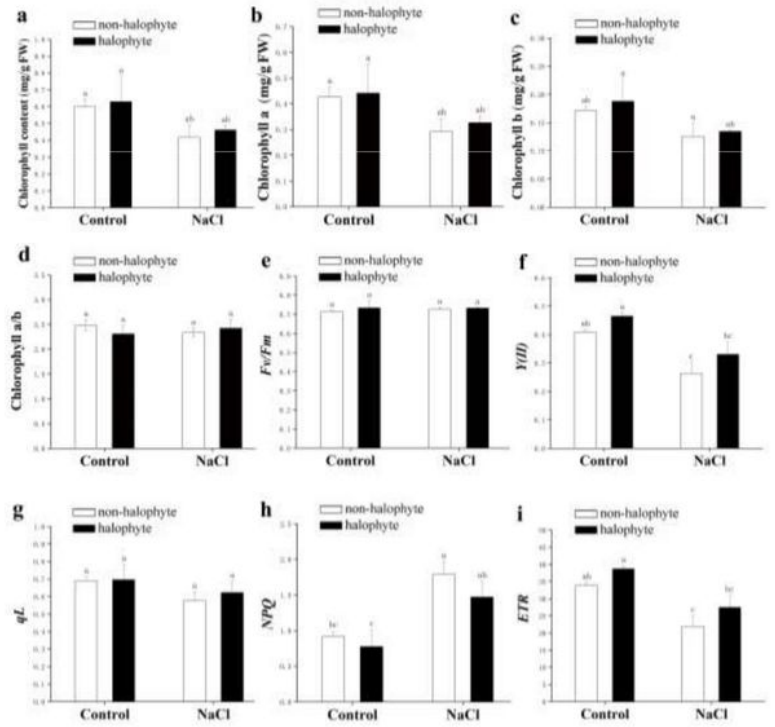

Fig. 3

Figure 3

The chlorophyll content and chlorophyll fluorescence parameters of the two lines under salts tress. **(a)**Chlorophyll (chl a + b). **(b)** Chlorophyll a. **(c)** Chlorophyll b.**(d)** Chlorophyll a/b. **(e)**Maximal efficiency of PSII photochemistry. **(f)** Actual quantum yield of PSII. **(g)** Photochemical quenching coefficient. **(h)** Non-photochemical quenching coefficient. **(i)** Electron transport rate. PSII, photosystem II. All the data represent the mean ± SD. The different letters in the bar graphs indicate significant differences at $P < 0.05$. SD, standard deviation.

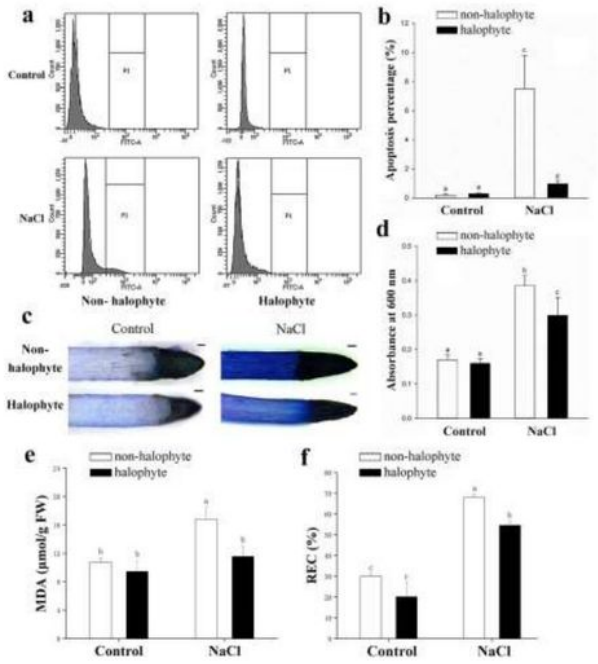

Fig. 4

Figure 4

The non-halophyte suffered more severe cell damage under salt stress than the halophyte. **(a-b)** Protoplast apoptosis under the salt treatment detected by Annexin V-FITC/PI double staining flow cytometry. **(a)** Flow cytometric estimation of apoptosis. **(b)** Representative flow cytometry histograms of the apoptosis. **(c-d)**Root cell membrane integrity detected by Evans blue staining. A darker stain indicated lower integrity. **(c)** Dead cells that were stained blue. **(b)**The degree of damage to the cell membrane. **(f)**

Malondialdehyde (MDA). (g)Relative electrical conductivity (REC). Bar=1 μm; All the data represent the mean ± SD. The different letters in the bar graphs indicate significant differences at $P < 0.05$. SD, standard deviation.

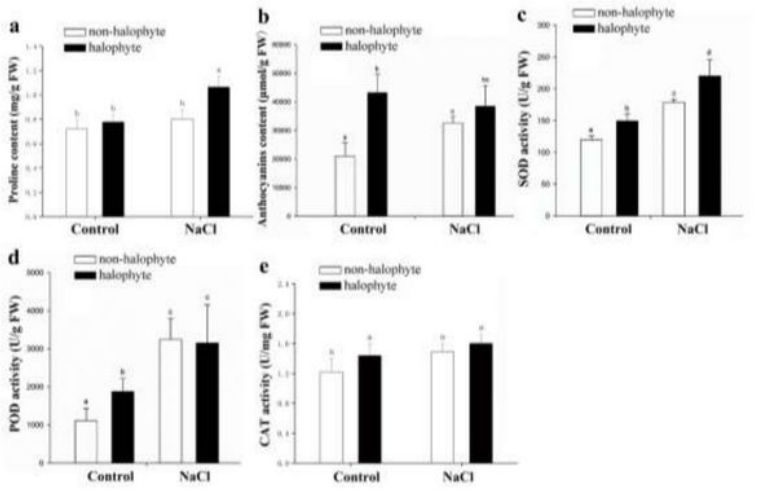

Fig. 5

Figure 5

Physiological changes induced by salt in the leaves of *Ipomoea cairica*. **(a)**Proline (PRO). **(b)** anthocyanin content. **(c)** Superoxide dismutase (SOD). **(d)** Peroxidase (POD). **(e)** Catalase (CAT). All the data represent the mean ± SD. The different letters in the bar graphs indicate significant differences at $P < 0.05$. SD, standard deviation.

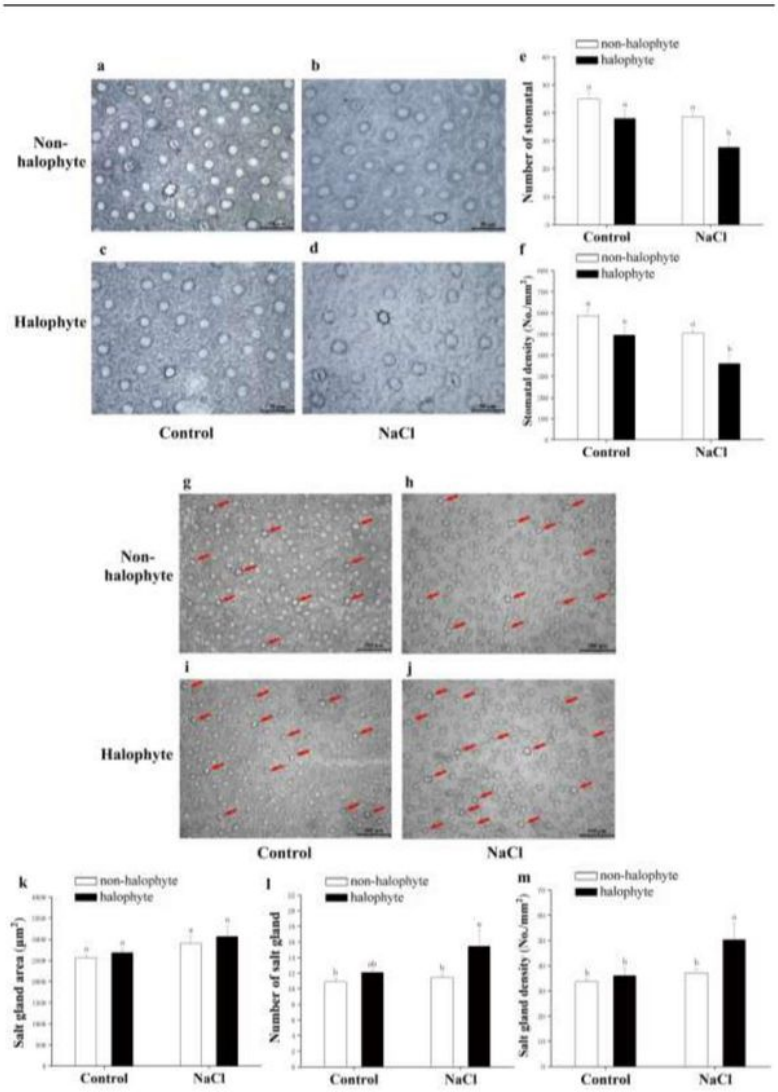

Fig. 6

Figure 6

Effect of NaCl concentrations on the stomata and salt glands of the two lines after 60 days. The bars indicate the salt gland density based on salt gland number per single leaf area (mm^2): **(a-d)** Stomata. **(e)** Number of stomata. **(f)** Stomatal density. **(g-j)** Salt glands are marked with red arrows. **(k)** Salt gland area. **(l)** Number of salt glands. **(m)** Salt gland density. Data are the means of 30 replicates (e, f, k l, m) ± SD. Different letters indicate a significant difference at $P < 0.05$. SD, standard deviation.

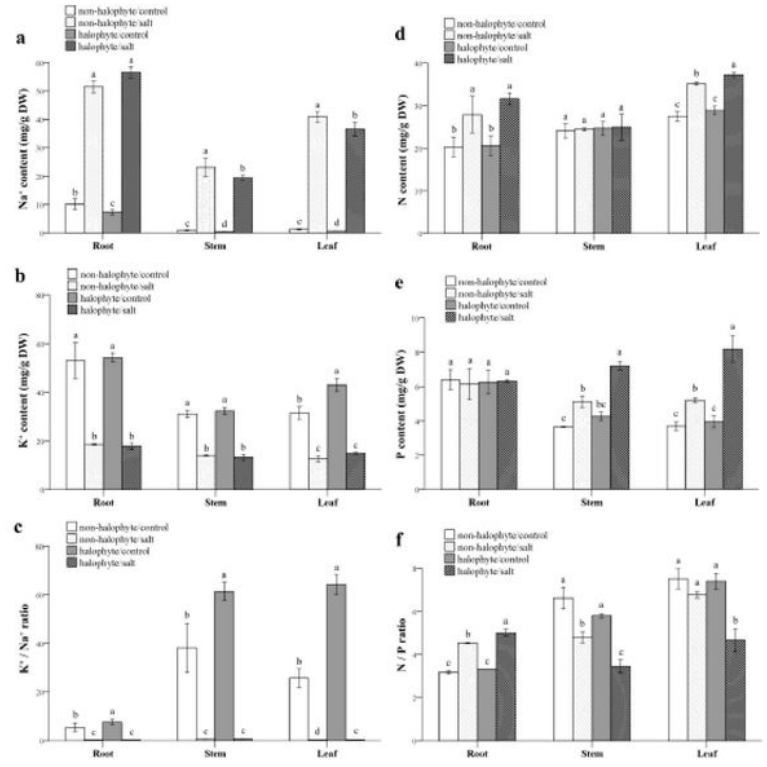

Fig. 7

Figure 7

The contents of elements and their allocation in the roots, stems and leaves of the halophyte were more balanced and conducive to growth than those of the non-halophyte under salt stress. (**a)** Sodium ion (Na^+) content. (**b)** Potassium ion (K^+) content. (**c)** K^+/Na^+ ratio. (**d)** Nitrogen (N) content. (**e)** Phosphorus (P) content. (**f**) N/P ratio. All the data represent the mean ± SD. The different letters in the bar graphs indicate significant differences at $P < 0.05$. SD, standard deviation.

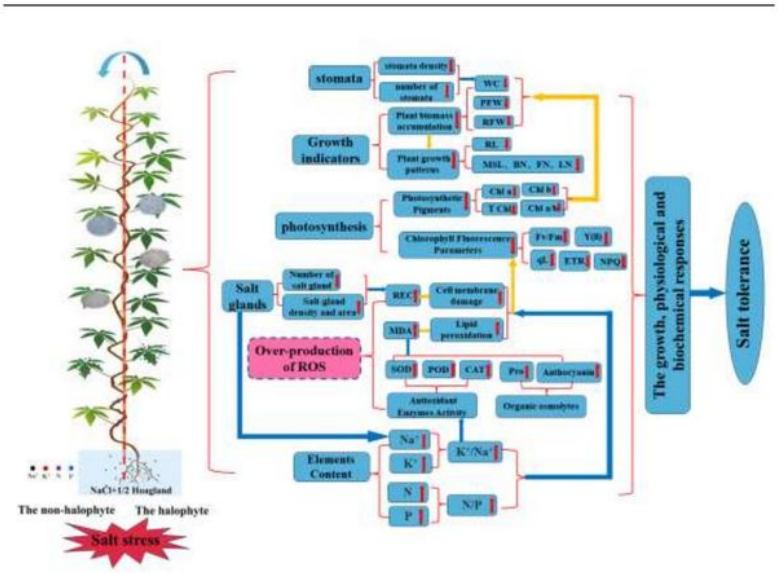

Fig. 8

Figure 8

Schematic representation of the inhibition of growth induced by salinity. WC, Water content; PFW, plant fresh weight; RFW, fresh weight of roots; RL, root length; MSL, main stem length; BN, branch number; FN, flower number; LN, leaf number; Chl a, chlorophyll a content; Chl b, chlorophyll b content; TChl, total chlorophyll content; Chl a/b, chlorophyll a/b; Fv/Fm, Maximal efficiency of PSII photochemistry; qL, Photochemical quenching coefficient; Y(II) Actual quantum yield of PSII; NPQ, Non-photochemical quenching coefficient; ETR, Electron transport rate; MDA, malondialdehyde; REC, relative electrical conductivity; Pro, proline; SOD, superoxide dismutase; POD, peroxidase. Na^+, sodium ion; K^+, potassium ion; K^+/Na^+ sodium and potassium ion ratio; N, Nitrogen; P, Phosphorus; N/P, Nitrogen and Phosphorus ratio.